ISBN: 978-3-95450-208-0 doi:10.18429/JACoW-IPAC2019-TUPGW091

LATTICE MEASUREMENTS OF THE APS INJECTOR RINGS *

V. Sajaev[†], C.-Y. Yao, Argonne National Laboratory, Lemont, USA

Abstract

APS Upgrade [1] will feature an entirely new storage ring, but will keep the existing injector complex consisting of the linear accelerator, Particle Accumulator Ring (PAR), and Booster. Due to the small dynamic aperture of the APS Upgrade lattice, swap-out injection [2–4] is adopted in which an entire old bunch is replaced with a new bunch. This injection method requires the Booster to provide high-charge bunches with up to 17 nC in a single bunch. Extensive work is being carried out on characterizing the existing injector rings to ensure future high-charge operation. In this paper, we will present results of the lattice measurement using the response matrix fit [5]. We will show the analysis of the achievable lattice measurement accuracy in the APS Booster and describe fit parameter modifications required to achieve good accuracy for the PAR.

APS BOOSTER

APS Booster [6] consists of 40 FODO cells with two dispersion-free sections for injection and extraction, has total length of 368 m, can accelerate electrons from 325 MeV to 7 GeV, and has a natural emittance of 130 nm at 7 GeV. Recently upgraded Beam Position Monitors (BPMs) [7] provide orbit readings in 10 time regions along the energy ramp cycle, with region 0 being right after injection and region 9 being immediately before extraction.

Orbit Response Matrix (ORM) fit was used to determine beta functions of the APS booster. The booster has 40 correctors and 80 BPMs in each plane, all of which were used for the ORM measurement. The ORM measurement program applies a corrector change in one time region and records the closed orbit in all regions. For each corrector, the program measures orbit at positive corrector change, zero, and negative corrector change. The response is then determined by fitting a straight line through these three points. The ORM was measured in four time regions: 0, 1, 3, and 8.

Looking at the rms of the measured ORM for all regions, one can determine the noise of the ORM measurement. Figure 1 shows the rms of the ORM. The four plots are for HX, HY, VX, and VY quadrants of the coupled response matrix, where H/V stands for the corrector plane (excitation plane) and X/Y stands for the BPM plane (response plane). For each curve, only one region – the excitation region – should have large rms, while the other regions should show the ORM measurement noise. One can see that, as expected, the noise is higher for the regions in the beginning of the ramp cycle: for example, the noise for region 0 is about 40 μm while it is below 10 μm for the final regions of the ramp.

* Work supported by the U.S. Department of Energy, Office of Science, Office of Basic Energy Sciences, under Contract No. DE-AC02-06CH11357.
† sajaev@anl.gov

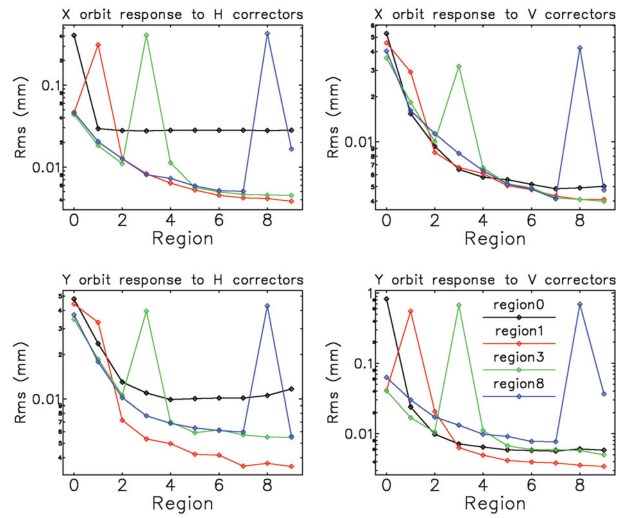

Figure 1: Rms of the overall ORM split into 4 parts by corrector and BPM plane. Every line corresponds to a single RM measurement, for which only one region is supposed to be non-zero; the rest is the measurement noise.

The ORM fit provides a set of quadrupole gradient errors and quadrupole tilts that best fit the measured ORM. They can also be used to calculate beta functions. The accuracy of the beta function determined this way is defined by the ORM measurement accuracy and the ORM fit accuracy. One way to determine the accuracy is to measure the ORM several times, process it, and then compare the resulting beta functions. Since we did not have several measurements under identical conditions, the following approach was used: the measured ORM was split into two by selecting two different subsets of correctors (this results in three matrices – full matrix and two half-matrices), and each matrix was fitted separately. The two half-matrix measurements are completely independent while the full-matrix measurement obviously overlaps with the other two measurements but still provides somewhat different data for the fit.

The ideal beta functions of the booster are typical FODO lattice beta functions varying between 2.5 and 16 m and can be found in [6]. Figure 2 (left) shows the beta function difference between the ideal lattice and the lattices resulting from the ORM fit of three different response matrices. Time region 3 is shown, other regions are similar. Using the results in Fig. 2, a standard deviation for every point along s was calculated and then averaged over s. Figure 2 (right) summarizes the standard deviation results for all measured regions. This standard deviation can be considered the beta function determination accuracy. However, since only three points were used to calculate the standard deviation, the result could be underestimated. For a Gaussian distribution sampled at three points, there is 20% chance of underesti-

ISBN: 978-3-95450-208-0 doi:10.18429/JACoW-IPAC2019-TUPGW091

mating the standard deviation by more than a factor of two, and 10% chance of underestimating it by a factor of three [8]. Still, even if possible underestimation is taken into account, the beta function determination is surprisingly good for a rapidly cycling booster.

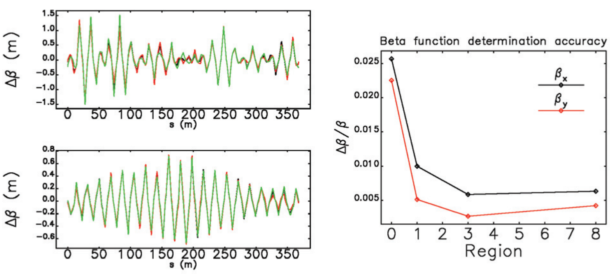

Figure 2: Left: Beta function difference between ideal lattice and models determined from three different ORM. Right: Beta function determination accuracy based on standard deviation between 3 different RM fits.

The booster vertical emittance is an important parameter that can affect the injection efficiency into the APS-U ring [9]. The vertical emittance can be determined from the skew quadrupole errors obtained in the ORM fit. The quality of the skew quadrupole fitting results were checked using the same approach of fitting subsets of correctors as was used for the beta function accuracy determination. Figure 3 (left) shows good agreement in vertical dispersion between three different fits for the region 8. However, the vertical emittance calculated with the 6D beam-moments method [10, 11] shows large disagreement, as seen in Fig. 3 (right). In addition, the values of the vertical emittance obtained from the fitted models are very small, they correspond to the emittance ratio of 1% or smaller. It is hard to believe that the coupling could be so small in a booster without any coupling correction.

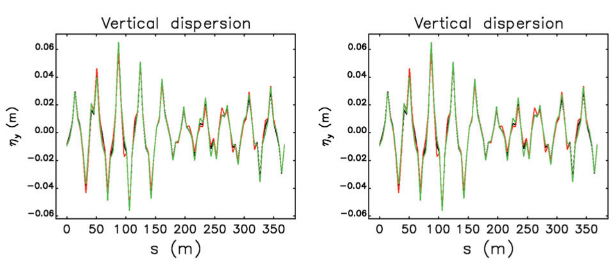

Figure 3: Left: Vertical dispersion as determined from three different RM subsets. Right: Corresponding vertical emittances.

Because of the unexpectedly small values of the vertical emittance, we sought to confirm the order of magnitude with a different calculation. It is clear that the larger the coupling, the larger the elements of the cross-plane (off-diagonal) ORM. Therefore, one can characterize the coupling by calculating the rms of all elements of the cross-plane ORM. The following procedure was followed to determine the vertical emittance: first, the rms of the overall measured cross-plane ORM was determined; second, many random sets of quadrupole tilts were generated and corresponding cross-plane response and vertical emittance were calculated; then the vertical emittance of the Booster was determined by comparing the measured and calculated rms cross-plane response.

To get a better estimate of the coupling strength using the rms of cross-plane response, one needs to subtract the effect of the BPM and corrector tilts from the measurements. Comparing the fitting results of the three ORM subsets, one can see that the determination of the BPM and corrector tilts is done with good accuracy. Therefore, subtraction of the BPM and corrector tilts is straightforward. The rms of the measured cross-plane response after subtracting BPM and corrector tilt effects was found to be 15 μm.

To simulate vertical emittance dependence on the rms cross-plane response, 1000 sets of random quadrupole tilts were generated, and the rms cross-plane response and vertical emittance were calculated for each set. Figure 4 (left) shows the results. Then, only the cases with rms cross-plane response between 14 and 16 μm were kept, and the cumulative distribution of the vertical emittance was calculated. Figure 4 (right) shows the result. Based on this result, the vertical emittance of the Booster is determined to be between 0.5 and 2.5 nm. It is interesting to note that the result shown earlier in Fig. 3 (right) actually falls within this range.

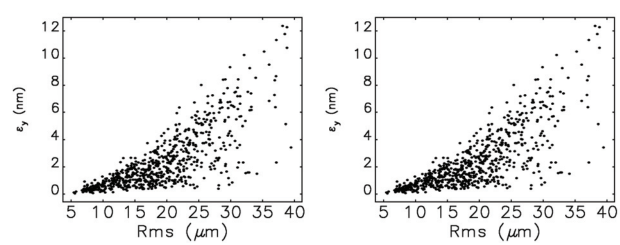

Figure 4: Left: Calculated vertical emittance as a function of the cross-plane rms response value. Right: CDF of the vertical emittance for the cases with cross-plane response rms value between 14 and 16 μm.

PAR LATTICE DETERMINATION

The APS Particle Accumulator Ring (PAR) is a 30.7-m-long, 450-MeV ring, that is used to accumulate and damp several bunches coming from the linac into one bunch and then deliver this bunch to the APS booster [12]. The interesting feature of the PAR is the absence of defocusing quadrupoles – the focusing in the vertical plane is provided only by the dipole edge focusing.

ORM was measured using a 5-point scan for each corrector. The accuracy of the slope determination gives equivalent orbit measurement accuracy of 2 μm at the maximum corrector excitation. The initial response matrix fit resulted in residual fit errors of 19 μm for HX, 1.6 μm for HY, 1.8 μm for VX, and 12 μm for VY. Clearly, the cross-plane ORM quadrants HY and VX are fitted down to the measurement

ISBN: 978-3-95450-208-0 doi:10.18429/JACoW-IPAC2019-TUPGW091

accuracy, while the diagonal quadrants HX and VY are far from the that.

Initial investigation of the lattice file immediately revealed a discrepancy: the lattice file has BPMs located at the ends of quadrupoles while in reality the BPMs are striplines that are located inside quadrupoles with only feedthroughs sitting outside of the quadrupoles. Besides BPM locations, there are several other candidates for the fit improvement: dipole edge field integral parameter FINT [11], dipole entrance and exit angles E1 and E2, and possibly quadrupole locations. All these parameters are not part of the standard ORM fit, so the fitting program had to be modified to include variation of arbitrary model parameters using a user supplied script.

Table 1 gives residual errors after the fit when different sets of special variables were used in addition to the standard set of quadrupoles, correctors, and BPMs. One can see that the BPM locations dominate the fit accuracy, while the dipole parameters do not have a significant effect.

Table 1: Residual Fit Errors and Relative Quadrupole Error RMS

	E1/E2	FINT	BPM shift	All 3	+ Quad posit.
Total (μm)	2.56	2.61	1.76	1.86	1.80
XX (μm)	3.62	3.63	1.95	2.05	2.01
XY (μm)	1.50	1.50	1.48	1.48	1.48
YX (μm)	1.68	1.68	1.67	1.67	1.67
YY (μm)	2.73	2.96	1.81	2.08	1.90
Quad RMS (%)	12	9.3	17	13	3.7

Analysis of the resulting fit variables revealed large and alternating quadrupole errors: pairs of Q1 and Q3 quadrupoles had almost opposite errors to the pairs of Q2 and Q4 quadrupoles. Looking at the PAR layout, one can see that Q1 and Q3 are located upstream of the dipoles and between dipoles and sextupoles, while Q2 and Q4 are located downstream of the dipoles with nothing on the downstream side of the quadrupoles. This asymmetry might result in longitudinal shift of the quadrupole centers. To account for that, longitudinal quadrupole position was added to the fit. Result of the fit with all special variables and quadrupole positions is also given in the Table 1 in the column "+Quad posit." One can see that adding quadrupole position fitting does not improve the accuracy of the fit, but it reduces the required quadrupole corrections significantly. Rms quadrupole correction strengths are shown in the last row of the table. Table 2 gives the values of the special variables obtained in the fit. Shifts of quadrupole centers seem large, but that is what minimized the quadrupole corrections needed to best fit the measured ORM.

Figure 5 compares measured beta functions and dispersion to the ideal lattice. The deviations from the ideal lattice are small for beta functions, but somewhat significant for horizontal dispersion.

Table 2: Values of the Special Variables Obtained in the Fit

E1 and E2	+0.004	relative to -0.448095
FINT	-0.07	relative to 0.40
BPM shift (P1/P3)	50 mm	relative to quad center
BPM shift (P2/P4)	0 mm	relative to quad center
Quad shift (Q1/Q3)	20 mm	towards the dipole
Quad shift (Q2/Q4)	20 mm	away from the dipole

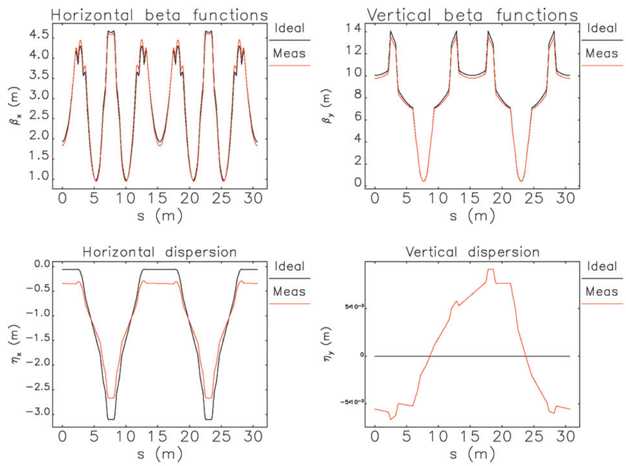

Figure 5: Ideal and "measured" beta functions and dispersion. "Measured" beta functions and dispersion are obtained from the fitted model.

CONCLUSION

We performed orbit response matrix fit for APS PAR and Booster. We determined that the rms beta function distortion for the Booster is below 5%, which is surprisingly small for a ring where no lattice correction was ever applied. The beta function determination accuracy for the booster is 1%, which is also unexpectedly accurate for the measurement during energy ramp. On a contrary note, the ORM accuracy was not enough to determine vertical emittance of the booster. We used rms cross-plane response as a proxy for the coupling and determined by comparing with simulations that the vertical emittance value is limited between 0.5 and 2.5 nm.

For the PAR, we had to modify the ORM fitting program to allow for varying of arbitrary parameters such as BPM and quadrupole positions and dipole edge field integral parameter and dipole entrance and exit angles. After these modifications, the fit was done almost to the measurement accuracy. The beta functions obtained from the fit were close to the ideal values.

REFERENCES

[1] M. Borland *et al.*, "The Upgrade of the Advanced Photon Source", in *Proc. IPAC'18*, Vancouver, Canada, Apr.-May 2018, pp. 2872–2877. doi:10.18429/JACoW-IPAC2018-THXGBD1

ISBN: 978-3-95450-208-0 doi:10.18429/JACoW-IPAC2019-TUPGW091

[2] R. Abela, W. Joho, P. Marchand, S. V. Milton, and L. Z. Rivkin, “Design Considerations for a Swiss Light Source (SLS)”, in *Proc. EPAC’92*, Berlin, Germany, Mar. 1992, pp. 486–489.

[3] L. Emery and M. Borland, “Possible Long-Term Improvements to the Advanced Photon Source”, in *Proc. PAC’03*, Portland, OR, USA, May 2003, paper TOPA014, pp. 256–258.

[4] A. Xiao, M. Borland, and C. Yao, “On-axis Injection Scheme for Ultra-Low-Emittance Light Sources”, in *Proc. NAPAC’13*, Pasadena, CA, USA, Sep.-Oct. 2013, paper WEPSM13, pp. 1076–1078.

[5] J. Safranek, “Experimental Determination of Storage Ring Optics Using Orbit Response Measurements”, *NIM* A 388, p. 27, 1997.

[6] S. V. Milton, “The APS Booster Synchrotron: Commissioning and Operational Experience”, in *Proc. PAC 1995*, p. 594.

[7] A. Pietryla *et al.*, in *Proc. PAC 2007*, paper FRPMN116, p. 4390, 2007.

[8] M. Borland, private communication.

[9] APS-U Preliminary Design Report, 4-1.10.3.

[10] K. Ohmi, K. Hirata, and K. Oide, “From the beam-envelope matrix to synchrotron-radiation integrals”, *Phys. Rev.* E 49, 751, 1994.

[11] M. Borland. ANL/APS LS-287, Advanced Photon Source, 2000.

[12] M. Borland, “Update on the Argonne Positron Accumulator Ring”, in *Proc. PAC 1993*, pp. 2028-2030, 1993.